

Diagnostic value of F-18 FDG PET/CT for local and distant disease relapse surveillance in surgically treated RCC patients: Can it aid in establishing consensus follow up strategy?

Mai Amr Elahmadawy¹, Mohamed Samy Saied Elazab², Soha Ahmed³, Mohamed Salama⁴

¹Nuclear Medicine Department, National Cancer Institute Cairo University, Cairo, Egypt

²Radiodiagnosis department National Cancer Institute, Cairo University, Egypt

³Clinical Oncologist in Clinical Oncology & nuclear Medicine Department, Aswan University, Children's Cancer Hospital, Egypt

⁴Surgical Oncology department National Cancer Institute, Cairo University, Egypt

[Received 30 V 2018; Accepted 3 VII 2018]

Abstract

BACKGROUND: Aim of the study was to evaluate the diagnostic performance of FDG PET-CT for the detection of local and distant disease relapse in surgically treated patients with renal cell carcinoma (RCC).

MATERIAL AND METHODS: This retrospective study includes 96 patients underwent FDG PET-CT scanning in the post-surgical follow up within the first 6–12 months referred to nuclear medicine department, to perform PET/CT study. Each patient underwent FDG PET-CT with low dose CT, followed immediately by full dose Ce-CT. Sites of the relapse were categorized into local and distant recurrence. Distant recurrence sites were divided into lymph nodes, lung, bone, and other soft tissue sites. The final diagnosis of disease status was made on subsequent follow up by conventional imaging (CT/MRI), FDG PET-CT, or histopathology whenever possible.

RESULTS: Local and/or distant disease relapse was confirmed in 69 (71.9%) patients and the rest 28.1% were free. Regarding local recurrence FDG PET-CT showed specificity of 100% compared to 98.6% with Ce-CT ($p > 0.05$) and higher sensitivity noted with Ce-CT (100%) compared to 96% with FDG PET-CT. For global distant sites of metastases Ce-CT revealed high sensitivity and NPV of 93.3% & 96.9% respectively yet lower specificity (93.96%) and PPV (87.5%) was seen with Ce-CT compared to 99.6% and 99.1% with FDG PET-CT respectively. The higher Ce-CT sensitivity was attributed to its ability to detected 100% of cases of lung metastases compared to 80.6% with FDG PET-CT (P -value < 0.05).

CONCLUSION: FDG PET-CT appears to be a very efficient tool in post-surgical surveillance of patients with RCC with notable ability to probe even uncommon sites of distant recurrence.

KEY words: RCC, FDG PET-CT, post-surgical surveillance, relapse

Nucl Med Rev 2018; 21, 2: 85–91

Introduction

Renal cell carcinoma (RCC) is the most common type of kidney cancer in adults, responsible for approximately 90–95% of cases, and represents 3% of all adult cancers [1]. It has been known for its resistant nature to chemo and radiotherapies, thus surgery (either

partial or total nephrectomy) remains the mainstay of localized disease treatment [2]. Surgically treated localized disease has favorable outcome with 5 years survival rate of 68.4%; however, 20–40% of patients developed local or distant disease relapse, lowering survival rate to less than 10% [3]. Moreover, recently, the oncogenic mechanism of RCC has been elucidated and drugs that target relevant biological pathways have been developed as sunitinib, sorafenib, multiple tyrosine kinase inhibitors (multiple TKIs) targeting vascular endothelial growth factor receptor (VEGFR), and everolimus [4, 5]. Therefore, postoperative planning and follow up in RCC are worthwhile with continuous evolution of recommendations for

Correspondence to: Mai Amr Elahmadawy, Nuclear Medicine Department, National Cancer Institute Cairo University, Cairo, Egypt, e-mail: mai_4a@yahoo.com

surveillance of patients with RCC [2]. The morphological diagnostic modalities Ultrasonography (US), contrast enhanced computed tomography (Ce-CT) and magnetic resonance imaging (MRI) are commonly used imaging modalities for the detection of RCC recurrences, however, a consensus surveillance protocol does not exist for follow-up of RCC after nephrectomy [2, 6]. RCC has been shown to metastasize to almost all soft tissues in the body, but most commonly to the lung, followed by bone, liver, brain, and local recurrence. Metastases to brain, bone, and liver often present as widely disseminated disease. Modalities of the survey are chosen to reflect the most prevalent locations of RCC recurrence. In addition, stringent surveillance to detect recurrences in areas most amenable to further therapy is paramount [7].

Although the role of FDG PET-CT in characterizing renal masses and diagnosing RCC is conflicting, the aggressive and often insidious nature of RCC reflected by its high recurrence rates can be probed by FDG PET-CT with its known ability to detect actively proliferating or aggressive disease in one setting whole body imaging [8]. Therefore, the aim of our study was to investigate the role of FDG PET-CT in the detection of local and distant disease relapse in patients who underwent nephrectomy for RCC in comparison to one of the traditional standard techniques which are (Ce-CT).

Material and methods

This retrospective study was conducted on 96 patients with RCC all pathologically confirmed after nephrectomy. The majority (78%) was of clear cell subtype, the remaining (22%) were of chromophobe and papillary cell subtypes. Patients were referred to the nuclear medicine unit in National Cancer Institute (NCI) and Children Cancer Hospital (CCH) to perform FDG PET-CT study, due to clinical suspicion of disease relapse, from 3rd February 2010 to 31st December 2015. Each patient underwent FDG PET-CT with low dose CT followed by a full dose Ce-CT study.

Inclusion criteria

- Patients with histologically proven renal cell carcinoma after surgical resection.
- Patients underwent FDG PET-CT scanning in the post-surgical follow up within the first 6–12 months after surgery to exclude (or confirm) local or distant disease relapse.

FDG PET-CT findings verified by histology and/or other imaging magnetic resonance imaging [MRI], or bone scan performed within a period of 1 month.

Availability of clinical follow-up data including multidisciplinary meeting reports, laboratory exams, and radiological exams as ultrasound examinations, ce-CT, MRI, FDG PET-CT, and bone scans, available for at least 6 months from the date of the first post-surgical FDG PET scan.

FDG PET-CT scans were retrospectively retrieved and reviewed by a nuclear medicine physician and correlated with ce-CT scans that were reviewed by radiodiagnosis physician.

PET-CT findings were interpreted as positive if the focal area of FDG uptake in the abdomen or outside the abdomen was more than the surrounding background tissue.

Ce-CT considered positive: in case of soft tissue lesions (local or distant); the presence of sizable lesions, the pattern of contrast

enhancement, reaching a pathological size (as in case of nodal involvement). In case of bone lesions; the presence of lytic or sclerotic changes.

The reference for results verification was based on:

- Histo-pathological data (if available)
- Clinico-laboratory assessment and follow-up data: were, otherwise, the reference.

FDG PET-CT scanning and image analysis

FDG PET-CT study was performed using a dedicated PET-CT scanner. This camera integrates a PET scanner with a dual-section helical CT scanner and allows the acquisition of co-registered CT and PET images in one session. All patients fasted for 6 hours before the injection of 370 MBq of 18 F-FDG. Scanning started 60 minutes after tracer injection (5–7 bed positions; acquisition time, 2–3 min/bed position). Blood glucose levels did not exceed 150 mg/dL. Initially, patients were examined in the supine position with arms elevated, and CT scanning was started at the level of skull base with the following parameters: 40 mAs; 130 kV; slice thickness, 2.5 mm; pitch, 1.5. The CT scans were acquired during shallow normal breathing and reached caudally to the mid thighs. PET over the same region was performed immediately after acquisition of the low dose CT images. CT-data were used for attenuation correction, and images were reconstructed as 3-mm slices applying a standard iterative algorithm (ordered-subset expectation maximization). Images were interpreted at a workstation equipped with fusion software that provides multi-planar reformatted images and enables display of the PET images, CT images, and fused PET-CT images in any percentage relation. Image interpretation was accomplished by two experienced nuclear medicine physicians and a radiologist. The analysis was performed using a multimodality computer platform. For semi-quantitative analysis, the nuclear medicine physicians referred to the PET-CT fusion images to set a spherical volume of interest (VOI) over the regions of interest and then recorded the maximum standardized uptake value (SUV max) in the VOI.

Contrast-enhanced CT scanning

CT scanning was performed using multi-detector CT scanner. Non-ionic iodinated contrast material (300 mgI/ml) at 2.0 ml per kilogram body weight was injected through antecubital vein with a total injection time of 30 seconds in principle via automated injector (based on the recent available kidney function tests).

Statistical analysis

All data were analyzed using SPSS 22.0 for Windows (SPSS Inc., Chicago, IL, USA) and MedCalc 13 for windows (MedCalc Software bvba, Ostend, Belgium). The trend of change in percent of ordinal categorical variables was compared using Chi-square test for trend. McNemar's test was used for comparison between paired data. The sensitivities, specificities, positive predictive values (PPV), negative predictive values (NPV), and accuracies were calculated. All tests were two-sided with $p < 0.05$ was considered statistically significant.

Written consents were routinely obtained from patients before studies and the local ethics committee has approved the evaluation of retrospectively collected patients' data.

Results

96 FDG PET-CT scans for 96 patients with pathologically proved RCC were retrospectively reviewed and analyzed. As regards the patients characteristics; males represented 65%, among our group and age group ranged from 37 to 70 years.

All available follow up data including blood tests, imaging, and biopsy results (when available) were used to confirm presence or absence of disease relapse as well as for monitoring therapy response. Accordingly, local and/or distant disease relapse was confirmed in 69 (71.9%) patients and the remaining 28.1% were totally free. Sites of the relapse were classified into 5 groups: local tumor

site, lymph nodes, lung, bone, and other soft tissue sites (brain, liver, adrenal, subcutaneous, intramuscular, and pancreas).

As regards Local recurrence detection patient based analysis for both FDG PET-CT & Ce-CT were performed. There is an overall comparable result with the same accuracy (98.95%) and higher sensitivity noted with Ce-CT (100%) compared to 96% with FDG PET-CT. Meanwhile, FDG PET-CT was able to exclude local tumor recurrence in one patient increasing its specificity to 100% compared to 98.6% with Ce-CT ($p > 0.05$) (Table 1, Fig. 1 and 2).

Table 1. Diagnostic performance of FDG PET-CT versus Ce-CT in detection of local tumor recurrence in patients with surgically treated RCC. (No. of patients = 96)

	FDG PET-CT	Ce-CT
TP	24	25
TN	71	70
FP	0	1
FN	1	0
SN	96%	100%
SP	100%	98.6%
NPV	98.6%	100%
PPV	100%	96.15%
Accuracy	98.95%	98.95%

TP — true positive, TN — true negative, FP — false positive, FN — false negative, SN — sensitivity, SP — specificity, NPV — negative predictive value, PPV — positive predictive value

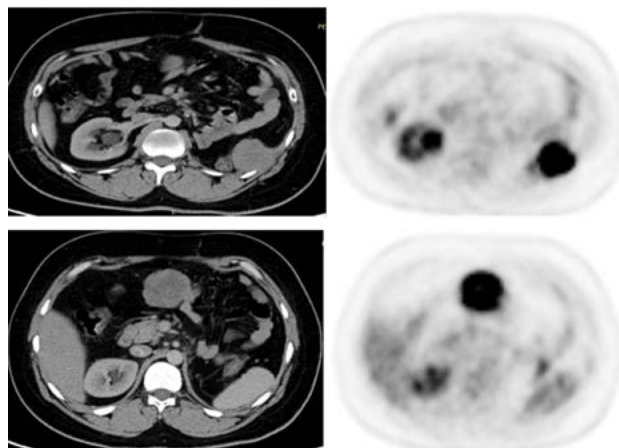


Figure 2. 38-years-old male patient underwent left nephrectomy for RCC, FDG PET-CT revealed FDG avid recurrent soft tissue mass at the operative bed SUVmax ~12.2, as well as large peritoneal deposit SUVmax ~10.2

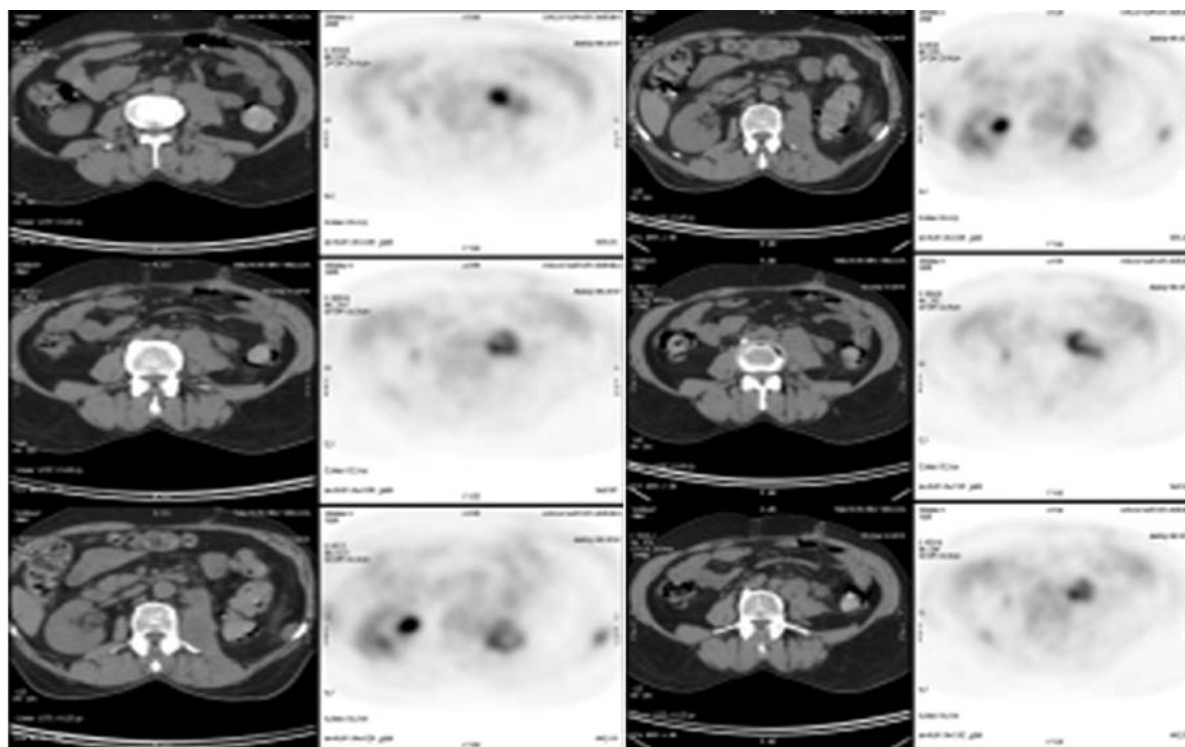


Figure 1. 56-years-old male patient with RCC underwent left nephrectomy with suspected recurrence, FDG PET-CT showed active mass infiltrating the left psoas muscle with SUVmax ~6.5, lumbar peritoneal nodule with SUVmax ~4.5 and common iliac nodal deposits with SUVmax ~9.5

Of the 96 studied patients, 63 had distant metastases with total number of 120 true positive sites of metastases, thus site based analysis was performed and higher incidence of false positive instances with distant metastases were reported in 16 patients with Ce-CT lowering its specificity (93.96%) and PPV (87.5%) compared to single false positive instance for FDG PET-CT with specificity and PPV of 99.6% and 99.1% respectively (p-value < 0.05).

On the other hand, slightly higher (yet still comparable) sensitivity and NPV shown by Ce-CT representing 93.3% and 96.9% respectively as compared to PET with sensitivity and NPV of 92.5% and 96.7% respectively. An overall higher diagnostic accuracy was revealed by PET/CT (97.4%) compared to Ce-CT (94%) yet no statistically significant difference (Table 2).

Furthermore, sites of distant metastases were classified as 4 main regions: lymph nodes, lung, bone, and other soft tissue sites (brain, liver, adrenal, subcutaneous, intramuscular, & pancreas). The analysis was performed comparing the diagnostic performance of both modalities at these different regions of distant metastases.

In our study 40 patients reveal true regional and/or distant nodal metastases, confirmed on follow up and/or histopathology, FDG PET-CT was able to detect nodal deposits with a sensitivity of 100% compared to 3 missed cases with Ce-CT with a sensitivity of 92.5%. Single false positive case reported with FDG PET-CT proved on histopathology to be reactive in nature (with specificity & PPV of 98.2% & 97.6% respectively), Meanwhile, considering size the determinant factor for CT interpretation, 3 cases were false positive by reaching pathological size on CT and proved to be of benign nature on follow up, lowering its specificity indices (Specificity & PPV) to 92.9 and 90.2% respectively. Higher overall diagnostic accuracy was observed with FDG PET-CT of 99% compared to 92.7% with Ce-CT (Table 3). It is worthwhile to note that true PET positive nodal cases showed wide range of variable degrees of metabolic activity with SUV max ranged from 1.7 to 20.3 (with mean value of 7.82), those active lesions also were of different sizes from 1 to 11.6 cm (positivity was not limited to pathological size).

Regarding lung metastases, as expected, full dose Ce-CT didn't miss a case with sensitivity of 100% compared to 80.6% for FDG PET-CT, which was statistically significant (P-value < 0.05). The cases that were truly positive on CT and missed by PET

were ≤ 12 mm in diameter. On the contrary, FDG PET-CT showed higher specificity, with all the detected cases truly positive and the average value for SUV max was 4.68, with specificity and PPV 100% compared to specificity & PPV of 93.8 & 88.6% with Ce-CT (Table 4).

FDG PET-CT showed optimum performance in both sensitivity and specificity indices reaching 100% in detection of bone metastases with SUV max ranged from 2 to 11.9 (average SUV max 4.6), whereas lower indices were noted with CT especially the PPV that was 87.5% with Ce-CT compared to 100% with PET/CT (p-value < 0.05) (Table 5, Fig. 3).

In our study, other soft tissue sites including the brain, liver, adrenal, subcutaneous, intramuscular, and pancreas were detected in 34 patients of the 96 patients. Higher diagnostic performance revealed by PET/CT with sensitivity, specificity, NPV, & PPV representing 91.2%, 100%, 95.4%, 100% and 96.9% respectively compared to 88.2%, 90.5%, 93.4%, 83.3% and 90.6% with Ce-CT, with statistical significance shown in PPV (P-value < 0.05) (Table 6, Fig. 4), The average value for SUV max was 7.15.

Discussion

RCC represents about 3% of adult malignancies. It is known for its variable natural history. Approximately 30% of case are metastatic

Table 3. Diagnostic performance of FDG PET-CT versus Ce-CT in detection of Nodal metastases in patients with surgically treated RCC. (No. of patients = 96)

	FDG PET-CT	Ce-CT
TP	40	37
TN	55	52
FP	1	4
FN	0	3
SN	100%	92.5%
SP	98.2%	92.9%
NPV	100%	94.5%
PPV	97.6%	90.2%
Accuracy	99%	92.7%

TP — true positive, TN — true negative, FP — false positive, FN — false negative, SN — sensitivity, SP — specificity, NPV — negative predictive value, PPV — positive predictive value

Table 2. Diagnostic performance of FDG PET-CT versus Ce-CT in detection of distant metastases in patients with surgically treated RCC. (No. of true metastatic sites = 120)

	FDG PET-CT	Ce-CT
TP	111	112
TN	263	249
FP	1	16
FN	9	8
SN	92.5%	93.3%
SP	99.6%	93.96%
NPV	96.7%	96.9%
PPV	99.1%	87.5%
Accuracy	97.4%	93.8%

TP — true positive, TN — true negative, FP — false positive, FN — false negative, SN — sensitivity, SP — specificity, NPV — negative predictive value, PPV — positive predictive value

Table 4. Diagnostic performance of FDG PET-CT versus Ce-CT in detection of Lung metastases in patients with surgically treated RCC. (No. of patients = 96)

	FDG PET-CT	Ce-CT
TP	25	31
TN	65	61
FP	0	4
FN	6	0
SN	80.6%	100%
SP	100%	93.8%
NPV	91.5%	100%
PPV	100%	88.6%
Accuracy	93.8%	95.8%

TP — true positive, TN — true negative, FP — false positive, FN — false negative, SN — sensitivity, SP — specificity, NPV — negative predictive value, PPV — positive predictive value

Table 5. Diagnostic performance of FDG PET-CT versus Ce-CT in detection of Bone metastases in patients with surgically treated RCC. (No. of patients = 96)

	FDG PET-CT	Ce-CT
TP	15	14
TN	81	79
FP	0	2
FN	0	1
SN	100%	93.3%
SP	100%	97.5%
NPV	100%	98.8%
PPV	100%	87.5%
Accuracy	100%	96.9%

TP — true positive, TN — true negative, FP — false positive, FN — false negative, SN — sensitivity, SP — specificity, NPV — negative predictive value, PPV — positive predictive value

Table 6. Diagnostic performance of FDG PET-CT versus Ce-CT in detection of Soft Tissue metastases in patients with surgically treated RCC. (No. of patients = 96)

	FDG PET-CT	Ce-CT
TP	31	30
TN	62	57
FP	0	6
FN	3	4
SN	91.2%	88.2%
SP	100%	90.5%
NPV	95.4%	93.4%
PPV	100%	83.3%
Accuracy	96.9%	90.6%

TP — true positive, TN — true negative, FP — false positive, FN — false negative, SN — sensitivity, SP — specificity, NPV — negative predictive value, PPV — positive predictive value

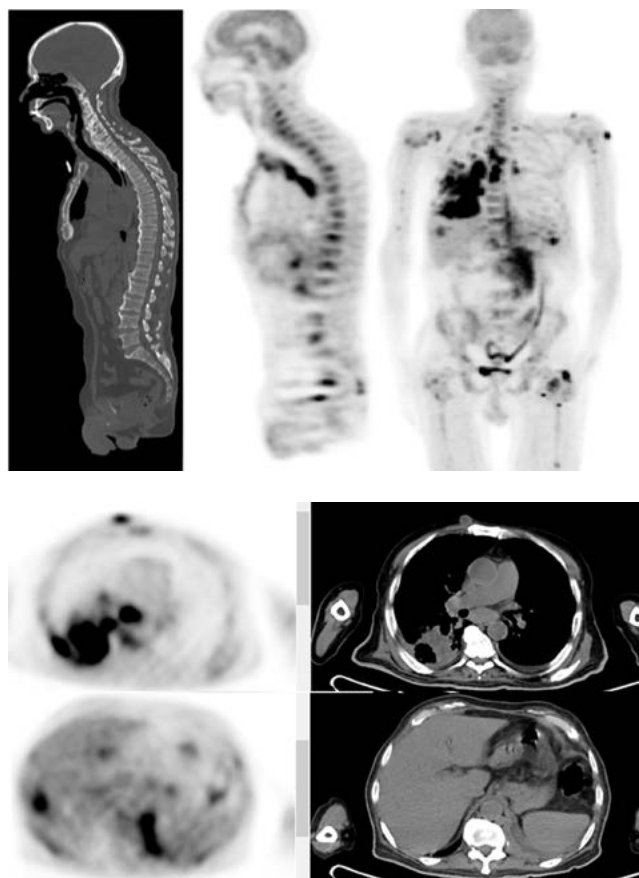


Figure 3. 68-years-old male patient underwent restaging FDG PET-CT, which revealed FDG avid metabolically active local tumor recurrence associated with FDG avid multiple nodal, hepatic, subcutaneous nodules, bilateral pulmonary nodules, and widespread bone/ bone marrow deposits. First row images could represent the absence of textural bone changes on CT images that appeared definitely infiltrated on PET images. Rest of images showed bilateral supraclavicular nodal involvement, active small right anterior chest wall nodule (easily missed on CT scanning alone), and active liver deposit

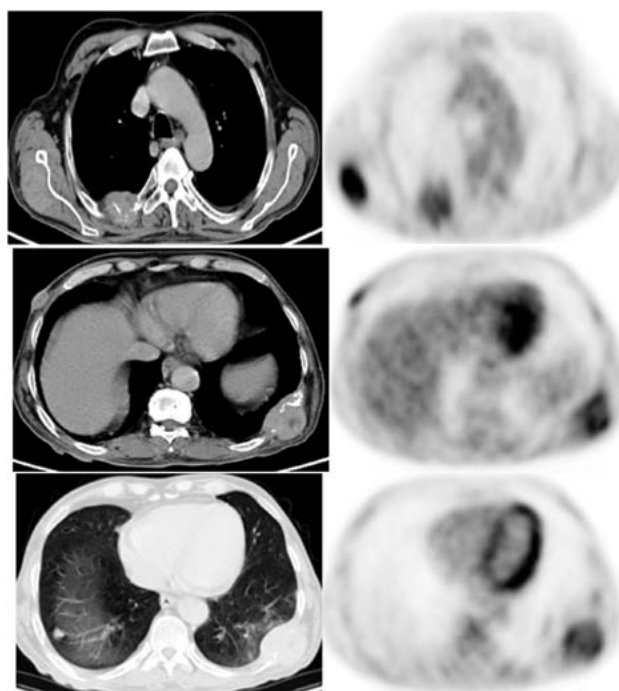


Figure 4. 62-years-old male patient underwent right radical nephrectomy and referred on clinical suspicion for recurrence. Images revealed metabolically active right infra-spinatus intramuscular lesion (1st row) and right chest wall subcutaneous soft tissue nodule (2nd row) with SUV max 6.5, multiple FDG avid destructive rib lesions associated with soft tissue component and NON-FDG avid lung nodules largest at right lower lobe (illustrated at the 3rd row images) measuring 1.2 cm

at the time of diagnosis and 20 to 40% develop metastases after radical nephrectomy [1, 3].

Disease recurrence, whether after partial or radical nephrectomy could be assessed by clinical suspicion and surveillance imaging. With the development of anti-angiogenesis targeted therapies, early detection of recurrence and proper disease surveillance become of

great interest [9, 10]. Up till now, no consensus has been reached for the pattern of follow up or disease surveillance and several authors have emphasized the need to individualize surveillance based on tumour stage, grade, tumour volume and type of surgery, whether partial or total nephrectomy [11].

Local recurrence after nephrectomy for RCC is uncommon. The prevalence has been reported to range between 1 and 2% in different series. Recurrent RCC after RN may be a result of metastatic disease within the ipsilateral adrenal gland, which was left in situ at the time of the primary surgery, inadequate excision of regional lymph nodes, or recurrent/residual disease in perirenal fatty tissue, in renal fossa, or within the psoas muscle. Inadvertent perioperative tumoral implantation may be another reason [12–14].

In the current study, comparable high diagnostic accuracy (98.95%) was noted with FDG PET-CT and Ce-CT, and FDG PET-CT was able to exclude local tumor recurrence in one patient increasing its specificity to 100% compared to 98.6% with Ce-CT ($p > 0.05$). Kumar et al. studied 63 patients who underwent 103 FDG PET-CT scans for evaluation of postsurgical RCC recurrence and reported sensitivity, specificity, and accuracy of 90%, 91%, and 90%, respectively [15]. Lower sensitivity (82%) and similar specificity (100%) was reported by Bertagna et al. [16], while lower sensitivity and specificity were reported by Alongi P et al., in a study done for the clinical role of FDG PET-CT in the restaging of RCC. For recurrent and/or metastatic lesions in 104 patients, FDG PET-CT demonstrated sensitivity and specificity of 74 and 80%, respectively [17].

In our study, Ce-CT revealed high sensitivity indices (93.3% and 96.9% for sensitivity and NPV respectively) but with high incidence of false positive instances with distant metastases reported in 16 patients lowering its specificity (93.96%) and PPV (87.5%) compared to single false positive instance for FDG PET-CT with specificity and PPV of 99.6% & 99.1% respectively (p -value < 0.05). Though other studies demonstrated variable FDG PET-CT sensitivity for detection of distant metastases (ranged from 63.6 to 90%, almost all illustrated specificity from 91 to 100%. Also, the additional information obtained from FDG PET influenced the course of therapeutic management in 11% of cases [18–21].

In our study, FDG PET-CT was able to detect nodal deposits with sensitivity of 100% compared to 92.5% with ce-CT. For CT, positivity is size dependent and reaching the pathological size stands behind the false positive cases and the relatively lower specificity of 92.9% as compared to FDG PET (98.2%). True PET positive nodal cases showed variable variability in metabolic activity with SUV max ranged from 1.7 to 20.3 (with a mean value of 7.82). Those active lesions ranged in size from 1 to 11.6 cm (positivity was not limited to pathological size). Other retrospective analysis by Win et al, reviewed the FDG PET-CT studies in 315 RCC patients with biopsy results. FDG PET-CT studies exhibited 100% sensitivity and 100% specificity in detecting all metastatic lesions of RCC, the smallest of which detected was a 7-mm lymph node [22].

Ce-CT optimum sensitivity for detection of lung metastases is well established. In our study reached 100% compared to 80.6% for FDG PET-CT which was statistically significant (P -value < 0.05). The cases that were truly positive on CT and missed by PET were ≤ 12 mm in diameter. However, the upper hand for specificity is still in favour of FDG PET-CT as all the detected cases were truly positive with the average value for SUV max was 4.68. In another study, Antonija et al. reported that the accuracy

of FDG PET-CT in metabolically active metastases is generally higher when compared to conventional CT except for identifying small lung deposits [23].

FDG PET-CT showed optimum performance with both sensitivity and specificity indices reaching 100% in detection of bone metastases with SUV max ranged from 2 to 11.9 (average SUV max 4.6), whereas lower indices were noted with CT, especially the PPV that was 87.5% with Ce-CT compared to 100% with FDG PET-CT (p -value < 0.05). This is comparable to the study done by Sharma et al; that concluded that FDG PET-CT showed similar accuracy for visualization of bone metastasis 93.7% [24].

Higher sensitivity and specificity indices were noted with FDG PET-CT with sensitivity, specificity, NPV, & PPV representing 91.2%, 100%, 95.4%, 100% and 96.9% respectively compared to 88.2%, 90.5%, 93.4%, 83.3% & 90.6% with Ce-CT. The false positive cases with CT were attributed to sizable adrenal nodules, however, MRI and follow up revealed their benign (adenomatous) nature, also small equivocal liver lesions that serial scans and follow-up reassure their stability over time and benign etiology. Regarding the CT false negative results, three out of the four cases had missed intramuscular involvement at different muscles groups and the fourth had few small subcutaneous nodules. All were obvious in PET images and one of the subcutaneous nodules was biopsied and its metastatic nature was histologically proven.

Conclusions

FDG PET-CT appears to be a very efficient tool in post-surgical surveillance of patients with RCC with notable ability to probe even uncommon sites of distant recurrence encouraging its introduction (together with complementary dedicated CT lung scanning protocol) to the follow-up protocol of post-surgically treated RCC patients. Meanwhile further larger scale studies with periodic follow up is recommended to support this role and to illustrate the optimum timing and frequency of FDG PET-CT imaging during follow up.

References

- Lam JS, Leppert JT, Belldegrun AS, et al. Novel approaches in the therapy of metastatic renal cell carcinoma. *World J Urol.* 2005; 23(3): 202–212, doi: [10.1007/s00345-004-0466-0](https://doi.org/10.1007/s00345-004-0466-0), indexed in Pubmed: [15812574](https://pubmed.ncbi.nlm.nih.gov/15812574/).
- Arnold IC, Lam JS, Figlin RA, et al. Surveillance Strategies for Renal Cell Carcinoma Patients Following Nephrectomy. *Rev Urol.* 2006; 8: 1–7.
- Krabbe LM, Bagrodia A, Margulis V, et al. Surgical management of renal cell carcinoma. *Semin Intervent Radiol.* 2014; 31(1): 27–32, doi: [10.1055/s-0033-1363840](https://doi.org/10.1055/s-0033-1363840), indexed in Pubmed: [24596437](https://pubmed.ncbi.nlm.nih.gov/24596437/).
- Rini BI, Hutson TE, Figlin RA, et al. Sunitinib versus interferon alfa in metastatic renal-cell carcinoma. *N Engl J Med.* 2007; 356(2): 115–124, doi: [10.1056/NEJMoa065044](https://doi.org/10.1056/NEJMoa065044), indexed in Pubmed: [17215529](https://pubmed.ncbi.nlm.nih.gov/17215529/).
- Escudier B, Eisen T, Stadler WM, et al. TARGET Study Group. Sorafenib in advanced clear-cell renal-cell carcinoma. *N Engl J Med.* 2007; 356(2): 125–134, doi: [10.1056/NEJMoa060655](https://doi.org/10.1056/NEJMoa060655), indexed in Pubmed: [17215530](https://pubmed.ncbi.nlm.nih.gov/17215530/).
- Reznek RH. CT/MRI in staging renal cell carcinoma. *Cancer Imaging.* 2004; 4 Spec No A: S25–S32, doi: [10.1102/1470-7330.2004.0012](https://doi.org/10.1102/1470-7330.2004.0012), indexed in Pubmed: [18215972](https://pubmed.ncbi.nlm.nih.gov/18215972/).
- Lam JS, Shvarts O, Leppert JT, et al. Surveillance following radical or partial nephrectomy for renal cell carcinoma. *Curr Urol Rep.* 2005; 6(1): 7–18, doi: [10.1007/s11934-005-0062-x](https://doi.org/10.1007/s11934-005-0062-x), indexed in Pubmed: [15610692](https://pubmed.ncbi.nlm.nih.gov/15610692/).
- Aide N, Cappele O, Bottet P, et al. Efficiency of [(18)F]FDG PET in characterising renal cancer and detecting distant metastases: a comparison with CT.

- Eur J Nucl Med Mol Imaging. 2003; 30(9): 1236–1245, doi: [10.1007/s00259-003-1211-4](https://doi.org/10.1007/s00259-003-1211-4), indexed in Pubmed: [12845486](https://pubmed.ncbi.nlm.nih.gov/12845486/).
9. Stephenson AJ, Chetner MP, Rourke K, et al. Guidelines for the surveillance of localized renal cell carcinoma based on the patterns of relapse after nephrectomy. *J Urol*. 2004; 172(1): 58–62, doi: [10.1097/01.ju.0000132126.85812.7d](https://doi.org/10.1097/01.ju.0000132126.85812.7d), indexed in Pubmed: [15201737](https://pubmed.ncbi.nlm.nih.gov/15201737/).
 10. Bjelogrić SK, Radulović S, Babović N. Molecular targeting agents in renal cell carcinoma: present strategies and future perspectives. *Curr Pharm Des*. 2008; 14(11): 1058–1077, doi: [10.2174/138161208784246252](https://doi.org/10.2174/138161208784246252), indexed in Pubmed: [18473855](https://pubmed.ncbi.nlm.nih.gov/18473855/).
 11. Escudier B, Porta C, Schmidinger M, et al. ESMO Guidelines Working Group. Renal cell carcinoma: ESMO Clinical Practice Guidelines for diagnosis, treatment and follow-up. *Ann Oncol*. 2014; 25 Suppl 3: iii49–iii56, doi: [10.1093/annonc/mdu259](https://doi.org/10.1093/annonc/mdu259), indexed in Pubmed: [25210086](https://pubmed.ncbi.nlm.nih.gov/25210086/).
 12. Eggener SE, Yossepowitch O, Pettus JA, et al. Renal cell carcinoma recurrence after nephrectomy for localized disease: predicting survival from time of recurrence. *J Clin Oncol*. 2006; 24(19): 3101–3106, doi: [10.1200/JCO.2005.04.8280](https://doi.org/10.1200/JCO.2005.04.8280), indexed in Pubmed: [16809736](https://pubmed.ncbi.nlm.nih.gov/16809736/).
 13. Schrodter S, Hakenberg OW, Manseck A, et al. Outcome of surgical treatment of isolated local recurrence after radical nephrectomy for renal cell carcinoma. *J Urol*. 2002; 167(4): 1630–1633, doi: [10.1097/00005392-200204000-00013](https://doi.org/10.1097/00005392-200204000-00013), indexed in Pubmed: [11912377](https://pubmed.ncbi.nlm.nih.gov/11912377/).
 14. Paparel P, Bigot P, Matillon X, et al. Local recurrence after radical nephrectomy for kidney cancer: management and prediction of outcomes. a multi-institutional study. *J Surg Oncol*. 2014; 109(2): 126–131, doi: [10.1002/jso.23473](https://doi.org/10.1002/jso.23473), indexed in Pubmed: [24174430](https://pubmed.ncbi.nlm.nih.gov/24174430/).
 15. Kumar R, Shandal V, Shamim SA, et al. Role of FDG PET-CT in recurrent renal cell carcinoma. *Nucl Med Commun*. 2010; 31(10): 844–850, doi: [10.1097/MNM.0b013e32833d6882](https://doi.org/10.1097/MNM.0b013e32833d6882), indexed in Pubmed: [20661166](https://pubmed.ncbi.nlm.nih.gov/20661166/).
 16. Bertagna F, Motta F, Bertoli M, et al. Role of F18-FDG-PET/CT in restaging patients affected by renal carcinoma. *Nucl Med Rev Cent East Eur*. 2013; 16(1): 3–8, doi: [10.5603/NMR.2013.0002](https://doi.org/10.5603/NMR.2013.0002), indexed in Pubmed: [23677757](https://pubmed.ncbi.nlm.nih.gov/23677757/).
 17. Alongi P, Picchio M, Zattoni F, et al. Recurrent renal cell carcinoma: clinical and prognostic value of FDG PET/CT. *Eur J Nucl Med Mol Imaging*. 2016; 43(3): 464–473, doi: [10.1007/s00259-015-3159-6](https://doi.org/10.1007/s00259-015-3159-6), indexed in Pubmed: [26268680](https://pubmed.ncbi.nlm.nih.gov/26268680/).
 18. Majhail NS, Urbain JL, Albani JM, et al. F-18 fluorodeoxyglucose positron emission tomography in the evaluation of distant metastases from renal cell carcinoma. *J Clin Oncol*. 2003; 21(21): 3995–4000, doi: [10.1200/JCO.2003.04.073](https://doi.org/10.1200/JCO.2003.04.073), indexed in Pubmed: [14581422](https://pubmed.ncbi.nlm.nih.gov/14581422/).
 19. Platzek I, Zastrow S, Deppe PE, et al. Whole-body MRI in follow-up of patients with renal cell carcinoma. *Acta Radiol*. 2010; 51(5): 581–589, doi: [10.3109/02841851003724846](https://doi.org/10.3109/02841851003724846), indexed in Pubmed: [20429759](https://pubmed.ncbi.nlm.nih.gov/20429759/).
 20. Aide N, Cappele O, Bottet P, et al. Efficiency of [(18)F]FDG PET in characterising renal cancer and detecting distant metastases: a comparison with CT. *Eur J Nucl Med Mol Imaging*. 2003; 30(9): 1236–1245, doi: [10.1007/s00259-003-1211-4](https://doi.org/10.1007/s00259-003-1211-4), indexed in Pubmed: [12845486](https://pubmed.ncbi.nlm.nih.gov/12845486/).
 21. Ljungberg B, Bensalah K, Bex A, et al. Guidelines on Renal Cell Carcinoma. *Eur Urol*. 2015; 67: 913–924.
 22. Win AZ, Aparici CM. Clinical effectiveness of (18)f-fluorodeoxyglucose positron emission tomography/computed tomography in management of renal cell carcinoma: a single institution experience. *World J Nucl Med*. 2015; 14(1): 36–40, doi: [10.4103/1450-1147.150535](https://doi.org/10.4103/1450-1147.150535), indexed in Pubmed: [25709543](https://pubmed.ncbi.nlm.nih.gov/25709543/).
 23. Antonija B, Jasna M, Marijana J, et al. PET/CT in renal and bladder cancers. *Arch Oncol*. 2012; 20: 97–102.
 24. Sharma P, Karunanithi S, Chakraborty PS, et al. 18F-Fluoride PET/CT for detection of bone metastasis in patients with renal cell carcinoma: a pilot study. *Nucl Med Commun*. 2014; 35(12): 1247–1253, doi: [10.1097/MNM.000000000000195](https://doi.org/10.1097/MNM.000000000000195), indexed in Pubmed: [25171438](https://pubmed.ncbi.nlm.nih.gov/25171438/).